

## Polymer electrolyte membranes based on poly(phenylene ether)s with sulfonic acid *via* long alkyl side chains†

Cite this: *J. Mater. Chem. A*, 2013, **1**, 11389

Xuan Zhang, Li Sheng, Teruaki Hayakawa, Mitsuru Ueda\* and Tomoya Higashihara\*

A series of poly(phenylene ether)s with sulfonic acid groups *via* long alkyl side chains, SPPEs, were successfully prepared as proton exchange membranes for fuel cells. The new monomer, bis[4-fluoro-3-(*p*-methoxybenzoyl)]biphenyl (**BFMBP**), containing two pendent methoxyphenyl groups was synthesized by the Friedel–Crafts reaction of 5-chloro-2-fluorobenzoyl chloride with anisole, followed by the nickel-mediated homocoupling reaction. Poly(phenylene ether)s (PPEs) were then successfully obtained by the aromatic nucleophilic substitution polycondensation of **BFMBP** with dihydroxy-monomers in the presence of potassium carbonate. Sulfonated PPEs (SPPEs) (IEC: 1.96–2.45 mequiv. g<sup>-1</sup>) could be prepared by the reaction of PPEs containing phenol units with 1,4-butanedisulfone. By the solution casting method, SPPEs produced transparent membranes with good mechanical properties, and showed good oxidative and dimensional stabilities, and high proton conductivities, e.g., 8.60 × 10<sup>-3</sup> S cm<sup>-1</sup> under 30% relative humidity at 80 °C, which is higher than that of Nafion 117.

Received 23rd May 2013

Accepted 22nd July 2013

DOI: 10.1039/c3ta12026k

www.rsc.org/MaterialsA

### Introduction

Polymer electrolyte membrane fuel cells (PEMFCs) have drawn worldwide attention because of their potential applications in transportation, stationary and portable electronics. PEMFC technology already provides sufficient performance to be competitive with alternative technologies in energy conversion applications. Polymer electrolyte membranes (PEMs) play an important role in the PEMFC system since they serve as a proton conductive carrier as well as the separator of the anode/cathode.<sup>1–26</sup>

Among the state-of-the-art PEMs, sulfonated perfluoropolymers (e.g., Dupont's Nafion®, 3M, and Aquivion® membranes), have been widely used in PEMFCs due to their high proton conductivity and high chemical stability. By chemical modifications or stabilizations, their new products (e.g., NRE212, PFIA, Aquivion™, etc.) could even withstand a high temperature of 120 °C.<sup>5</sup> However, some other notable drawbacks, such as a harsh manufacturing process, high cost, and fluoro-release problem still more or less restrict their practical use. Hence, a number of non-fluorinated acid ionomers, especially the sulfonated aromatic hydrocarbon polymers, have been widely studied as a branch of alternate PEMs. The typical materials used for these PEMs, such as sulfonated poly(ether ketone)s

(SPEKs),<sup>11,12</sup> sulfonated poly(arylene ether sulfone)s (SPAESs),<sup>16,17</sup> sulfonated polyimides (SPIs),<sup>18</sup> sulfonated poly(phenylene)s (SPPs),<sup>19–21</sup> sulfonated poly(phenylene ether)s (SPPEs),<sup>22–25</sup> etc., have been well developed during the past two decades.

Typical SPPEs are prepared by the sulfonation of the precursor poly(phenylene ether)s (PPEs). The phenylene rings in the main chain provide a high electron density and could be easily functionalized by sulfuric acid, chlorosulfonic acid, etc. For instance, Xu's group reported a series of SPPEs.<sup>24</sup> By blending SPPEs with brominated PPE, their membranes showed a higher fuel cell performance than Nafion. However, the sulfonic acid groups were directly located on the main chain, *ortho* to the “–O–” linkages, which might decrease the oxidative stability of these polymers. Unfortunately, no further information on their durability was presented by the authors. Watanabe's group previously prepared a series of SPPEs using the sulfonated alkoxy side chains as pendants.<sup>25</sup> Unlike the situation of SPPEs described above, the fairly low polarity of the main chain with a high polarity side chain produced problems regarding the solubility for such types of SPPEs. The as-prepared polymers became insoluble once they were recovered from the solution. Therefore, the authors treated them with tetrabutylammonium tetrafluoroborate. The resulting polymers with an ammonium-form could finally dissolve in benzyl alcohol and produce the membranes.

The polymers with flexible ether and rigid phenyl–phenyl linkages in the main chains are promising candidates for PEM designs, since they could support polymers with good toughness as well as high chemical stability. The issue lies in where to functionalize the sulfonic acid groups in order to satisfy the

Department of Organic and Polymeric Materials, Tokyo Institute of Technology, 2-12-1-H120, O-okayama, Meguro-ku, Tokyo 152-8552, Japan. E-mail: mueda@kanagawa-u.ac.jp; thigashihara@yz-yamagata-u.ac.jp; Fax: +81-3-5734-2127

† Electronic supplementary information (ESI) available. See DOI: 10.1039/c3ta12026k

requirements for solubility and proton conductive capacity. Our previous study showed interesting results such that the introduction of flexible alkyl sulfonated side chains to the random polymer main chains improved the proton conductivity at a low relative humidity (RH) due to the phase separation between the hydrophilic and hydrophobic domains, and the oxidative stability of membranes was also increased due to the location of the sulfonic acid groups far from the main chains, where oxy and peroxy radicals might be preferably formed.<sup>20,26</sup> However, the mechanical stability of these membranes was not sufficient for fuel cell applications. Therefore, in this study, the more robust poly(phenylene ether) was selected as the polymer main chain.

We now report a novel type of PPEs with long alkyl sulfonic acids, which were synthesized from a new monomer of bis[4-fluoro-3-(4'-methoxybenzoyl)]biphenyl (**BFMBP**) and various dihydroxy-monomers *via* aromatic nucleophilic substitution polycondensation and demethylation, followed by the reaction of the resulting polymers having phenol groups with 1,4-butanediol. Their properties, such as ion exchange capacity (IEC), water uptake (WU), dimensional change, mechanical properties, proton conductivities and morphology, were investigated in detail.

## Experimental section

### Materials

5-Chloro-2-fluorobenzoic acid, anisole, and  $\text{AlCl}_3$  were purchased from TCI and used as received. Thionyl chloride was purchased from Wako Pure Chemical Industries, Ltd and used as received. Bis(triphenylphosphino)nickel(II) ( $\text{Ni}(\text{PPh}_3)_2\text{Cl}_2$ , TCI) and tetraethylammonium iodide ( $\text{Et}_4\text{NI}$ , TCI) were dried at 100 °C under vacuum prior to use. Zinc powder was purchased from Aldrich, washed with 2.0 M hydrochloric acid, deionized water, ethanol, and diethylether, successively, and dried at 100 °C for 6 h and at room temperature for 18 h under vacuum. Tetrahydrofuran (THF, dehydrated, stabilizer-free, 99.5%, Wako) was refluxed over sodium benzophenone under  $\text{N}_2$  for 2 h, and then distilled just before use. *N,N*-Dimethylacetamide (DMAc, Wako) was dried over  $\text{CaH}_2$ , distilled under reduced pressure and stored over 4 Å molecular sieves prior to use. Other solvents and reagents were used as received.

### Synthesis of 5-chloro-2-fluoro-4'-methoxybenzophenone (CFMB)

To a 50 mL flask equipped with a magnetic stirrer, 5-chloro-2-fluorobenzoic acid (12.5 g, 71.6 mmol) and 20.0 mL of thionyl chloride were added. The solution was kept at 85 °C for 10 h and the excessive thionyl chloride was then evaporated. 5-Chloro-2-fluorobenzoyl chloride (**CFBC**) was obtained by evaporating under reduced pressure to afford a colorless liquid; 12.8 g (yield: 92%).  $^1\text{H NMR}$  ( $\text{CDCl}_3$ , ppm):  $\delta = 8.07\text{--}8.04$  (m, 1H, Ar-H),  $\delta = 7.62\text{--}7.57$  (m, 1H, Ar-H),  $\delta = 7.19\text{--}7.13$  (t,  $J = 8.7$  Hz, 1H, Ar-H).

To a fully dried 100 mL three-necked flask,  $\text{AlCl}_3$  (9.12 g, 68.4 mmol) and anisole (90.0 mL) were charged. After cooling to 0 °C by an ice-water bath, **CFBC** (12.0 g, 62.2 mmol) was added

dropwise to the mixture through a pressure-equilibrium drop funnel and the reaction mixture was then heated to 50 °C for 3 h. The solution was poured into ice water with a few drops of HCl, and the product was extracted with chloroform. After drying over  $\text{MgSO}_4$ , evaporation, and recrystallization from ethanol, **CFMB** (12.5 g) was obtained; yield: 76%. IR (KBr):  $\nu$  2960–2870 (C–H), 1647 (C=O), 1597 (C=C), 1180  $\text{cm}^{-1}$  (C–O–C).  $^1\text{H NMR}$  ( $\text{CDCl}_3$ , ppm):  $\delta = 7.81\text{--}7.78$  (d,  $J = 8.7$  Hz, 2H, Ar-H),  $\delta = 7.47\text{--}7.40$  (m, 2H, Ar-H),  $\delta = 7.12\text{--}7.06$  (t,  $J = 8.4$  Hz, 1H, Ar-H),  $\delta = 6.95\text{--}6.92$  (d, 2H,  $J = 8.7$  Hz, Ar-H),  $\delta = 3.87$  (s, 3H,  $-\text{OCH}_3$ ).  $^{13}\text{C NMR}$  ( $\text{CDCl}_3$ , ppm):  $\delta = 190.24$  (1C, C7), 164.18 (1C, C11), 159.73, 156.40 (1C, C4), 132.31 (1C, C2), 132.25, 132.14 (1C, C1), 130.03, 129.99 (2C, C9), 129.59, 129.54 (1C, C5), 129.50 (1C, C8), 128.89, 128.65 (1C, C6), 117.76, 117.45 (1C, C3), 113.86 (2C, C10), 55.53 (1C, C12). Anal. calcd for  $\text{C}_{14}\text{H}_{10}\text{ClFO}_2$ : C: 63.53; H: 3.81. Found: C: 63.58; H: 3.90%.

### Synthesis of bis[4-fluoro-3-(4'-methoxybenzoyl)]biphenyl (BFMBP)

To a 50 mL two-necked flask equipped with a magnetic stirrer were charged **CFMB** (5.00 g, 18.9 mmol),  $\text{Ni}(\text{PPh}_3)_2\text{Cl}_2$  (1.24 g, 1.89 mmol),  $\text{Et}_4\text{NI}$  (0.486 g, 1.89 mmol) and zinc dust (3.71 g, 56.7 mmol). After being exchanged with argon three times, 38.0 mL of anhydrous THF was added. The reaction mixture underwent a color change from green to yellowish brown and finally dark red at 50 °C for 24 h. After filtration, the product was separated by a silica column using  $\text{CH}_2\text{Cl}_2$  as an eluent. By recrystallization from ethanol, **BFMBP** (2.05 g) was obtained as white needle-like crystals; yield: 46%. IR (KBr):  $\nu$  2960–2870 (C–H), 1647 (C=O), 1600 (C=C), 1180  $\text{cm}^{-1}$  (C–O–C).  $^1\text{H NMR}$  ( $\text{CDCl}_3$ , ppm):  $\delta = 7.83\text{--}7.80$  (d,  $J = 9.0$  Hz, 4H, Ar-H),  $\delta = 7.66\text{--}7.62$  (m, 4H, Ar-H),  $\delta = 7.22\text{--}7.16$  (t,  $J = 9.0$  Hz, 2H, Ar-H),  $\delta = 6.93\text{--}6.90$  (d,  $J = 9.0$  Hz, 4H, Ar-H),  $\delta = 3.84$  (s, 6H,  $-\text{OCH}_3$ ).  $^{13}\text{C NMR}$  ( $\text{CDCl}_3$ , ppm):  $\delta = 191.51$  (2C, C7), 164.05 (2C, C11), 161.03, 157.69 (2C, C4), 135.78, 135.74 (2C, C1), 132.30 (2C, C2), 130.98, 130.86 (4C, C9), 129.91 (2C, C8), 128.87, 128.82 (2C, C6), 128.04, 127.82 (2C, C5), 116.90, 116.61 (2C, C3), 113.81 (4C, C10), 55.51 (2C, C12). Anal. calcd for  $\text{C}_{28}\text{H}_{20}\text{F}_2\text{O}_4$ : C: 73.36; H: 4.40. Found: C: 73.03; H: 4.72%.

### Synthesis of poly(phenylene ether) (2)

A typical procedure for the preparation of polymer **2b** is as follows. A three-necked flask was charged with **BFMBP** (1.20 g, 2.62 mmol), bisphenol (0.487 g, 2.62 mmol),  $\text{K}_2\text{CO}_3$  (0.416 g, 3.01 mmol), DMAc (8.40 mL) and toluene (8.00 mL). The mixture was purged with nitrogen and then heated to 140 °C for 2 h. After toluene was fully removed, the reaction temperature was gradually risen to 165 °C and kept for another 6 h. The resulting viscous solution was cooled down to room temperature, diluted with 8.40 mL of DMAc, and precipitated into methanol containing a few drops of concentrated HCl. The polymer was reprecipitated from 5 wt% DMF solution into a mixture solution ( $\text{CHCl}_3$ –methanol = 2/8). After drying at 100 °C under vacuum for 12 h, the fibrous polymer was obtained (1.23 g, yield: 77%). IR (KBr):  $\nu$  2960–2870 (C–H), 1658 (C=O), 1597 (C=C), 1169  $\text{cm}^{-1}$  (C–O–C).  $^1\text{H NMR}$  ( $\text{DMSO}-d_6$ , ppm):

$\delta = 7.87\text{--}7.77$  (bm, Ar-H),  $\delta = 7.52$  (bs, Ar-H),  $\delta = 7.14\text{--}6.96$  (bm, Ar-H),  $\delta = 3.82$  (s,  $-\text{OCH}_2-$ ).

### Synthesis of poly(phenylene ether) (3)

A typical synthetic procedure for the preparation of polymer **3b** is as follows. To a 200 mL three-necked flask equipped with a nitrogen inlet/outlet were charged polymer **2b** (1.00 g, 1.65 mmol) and  $\text{CH}_2\text{Cl}_2$  (80.0 mL). The solution was cooled to 0 °C in an ice bath, and a  $\text{BBr}_3/\text{CH}_2\text{Cl}_2$  solution (12.0 mL) was added dropwise to the solution. After addition, the reaction was kept at room temperature overnight. The resulting copolymer was obtained by carefully pouring the solution into water, filtered, washed thoroughly with water, and methanol, successively, and dried under vacuum at 80 °C for 12 h. Yield: 0.912 g (96%). IR (KBr):  $\nu$  3500–3200 ( $-\text{OH}$ ), 2960–2870 (C–H), 1643 (C=O), 1597 (C=C), 1169  $\text{cm}^{-1}$  (C–O–C).  $^1\text{H}$  NMR (DMSO- $d_6$ , ppm): 10.36 (s,  $-\text{OH}$ ),  $\delta = 7.87\text{--}7.67$  (bm, Ar-H),  $\delta = 7.34\text{--}7.26$  (bm, Ar-H),  $\delta = 7.10\text{--}6.99$  (bm, Ar-H),  $\delta = 6.86\text{--}6.64$  (bm, Ar-H).

### Synthesis of sulfonated poly(phenylene ether) (4)

A typical synthetic procedure for the preparation of polymer **4b** is as follows. To a 20 mL three-necked flask equipped with a nitrogen inlet/outlet were charged polymer **3b** (0.80 g, 1.39 mmol), sodium hydride (0.050 g, 2.08 mmol) and dimethyl sulfoxide (DMSO) (15.0 mL). The solution was heated to 100 °C and 1,4-butanediol (0.756 g, 5.45 mmol) was added dropwise to the mixture. After 12 h, the solution was cooled to room temperature and slowly poured into ethanol. The sulfonated copolymer was filtered and then dried in a vacuum oven at 100 °C for 12 h. Yield: 1.14 g (97%). IR (KBr):  $\nu$  2960–2870 (C–H), 1658 (C=O), 1600 (C=C), 1176  $\text{cm}^{-1}$  (C–O–C), 1119, 1049  $\text{cm}^{-1}$  (O=S=O).  $^1\text{H}$  NMR (DMSO- $d_6$ , ppm):  $\delta = 7.77\text{--}6.80$  (bm, Ar-H),  $\delta = 3.91$  (s,  $-\text{OCH}_2-$ ),  $\delta = 2.54$  (s,  $-\text{CH}_2-\text{SO}_3\text{Na}$ ),  $\delta = 1.84\text{--}1.74$  (m,  $-\text{CH}_2-$ ).

### Preparation of polymer 4 membranes

Membranes were prepared by a solution casting method. Polymer **4** was dissolved in DMSO with a concentration of 5% (m/v). After filtration, the solution was cast onto a clean Petri dish, dried at 80 °C for 20 h under atmosphere. The membrane was detached from the dish by immersing into water to remove the residual solvent, followed by soaking in 2 M  $\text{H}_2\text{SO}_4$  at 50 °C for 72 h for proton exchange. Then, the membrane was thoroughly washed with Milli-Q water. The thickness of the membrane was controlled to be about 50  $\mu\text{m}$ .

### Characterizations

$^1\text{H}$  (300 MHz) and  $^{13}\text{C}$  (75 MHz) NMR spectra were recorded on a Bruker DPX300S spectrometer using  $\text{CDCl}_3$  or DMSO- $d_6$  as the solvent and tetramethylsilane as the reference. Fourier transform-infrared (FT-IR) spectra were obtained with a Horiba FT-120 Fourier transform spectrophotometer. Number- and weight-average molecular weights ( $M_n$  and  $M_w$ ) were measured by gel permeation chromatography (GPC) on a Hitachi LC-7000 system equipped with polystyrene gel columns (TSKgel

GMHHR-M) eluted with *N,N*-dimethylformamide (DMF) containing 0.01 M LiBr at a flow rate of 1.0  $\text{mL min}^{-1}$  calibrated by standard polystyrene samples. Thermogravimetric analysis (TGA) was measured in  $\text{N}_2$  on a Seiko EXSTAR 6000 TG/DTA 6300 thermal analyzer at a heating rate of 10 °C  $\text{min}^{-1}$ . Dynamic mechanical analysis (DMA) was performed on the film specimens (length, 30 mm; width, 10 mm; thickness, 50  $\mu\text{m}$ ) by using the Seiko DMS 6300 at a heating rate of 2 °C  $\text{min}^{-1}$  with a load frequency of 1 Hz under a nitrogen atmosphere. The mechanical properties of SPPE membranes were also analyzed by tensile measurement, which was performed with a universal testing instrument (AGS-X 349-05489A, Shimadzu, Japan) at 20 °C and around 50% RH at a crosshead speed of 2  $\text{mm min}^{-1}$ . Wide-angle X-ray diffraction (WAXD) measurements were performed at ambient temperature by using a Rigaku-Denki UltraX-18 X-ray generator with monochromic Cu  $K_\alpha$  radiation (40 kV, 50 mA) from a graphite crystal of monochromator and a flat-plate type of imaging plate. Tapping mode atomic force microscope (AFM) images were taken by using a Seiko Instruments SPA-400 with a stiff cantilever of Seiko Instruments DF-20.

### Water uptake and dimensional change

The humidity dependence of water uptake was measured by placing the membrane in a thermo-controlled humid chamber for 4 h under each RH condition. The membrane was then taken out, and quickly weighed on a microbalance. Water uptake (WU) was calculated according to eqn (1):

$$\text{WU} = (W_s - W_d)/W_d \times 100 \text{ wt\%} \quad (1)$$

where  $W_s$  and  $W_d$  are the weights of wet and dried membranes, respectively.

For dimensional change measurements, squared membrane sheets were placed in a thermo-controlled humid chamber for 2 h under each RH condition. The dimensional change in the membrane thickness direction ( $\Delta t_c$ ) and the plane direction ( $\Delta l_c$ ) was calculated from eqn (2):

$$\Delta t_c = (t - t_s)/t_s, \Delta l_c = (l - l_s)/l_s \quad (2)$$

where  $t_s$  and  $l_s$  refer to the thickness and diameter of the membrane equilibrated at about 30 °C/30% RH, respectively;  $t$  and  $l$  refer to those of the membrane under each condition.

### Ion exchange capacity

IECs of the membranes were determined by a titration method. The proton-type samples were ion-exchanged by 15 wt% NaCl solutions and titrated with a 0.02 M NaOH solution with phenolphthalein as the indicator. The IEC was calculated from eqn (3):

$$\text{IEC} = C_{\text{NaOH}} \times V_{\text{NaOH}}/W_d \quad (3)$$

where  $C_{\text{NaOH}}$  and  $V_{\text{NaOH}}$  are the concentration of NaOH solution and the consumed volume of NaOH solution, respectively.

## Water sorption ( $\lambda$ )

The  $\lambda$  value was calculated from eqn (4):

$$[\text{H}_2\text{O}]/[\text{SO}_3^-] = \text{WU} \times 10/18 \times \text{IEC} \quad (4)$$

## Proton conductivity

Proton conductivity in the plane direction of the membrane was determined using an electrochemical impedance spectroscopy technique over the frequency from 5 Hz to 1 MHz (Hioki 3532-80). A two-point probe conductivity cell with two platinum plate electrodes was fabricated. The cell was placed in a thermo-controlled humid chamber at 80 °C for 2 h before the measurement. Proton conductivity ( $\sigma$ ) was calculated from eqn (5):

$$\sigma = d/(t_s w_s R) \quad (5)$$

where  $d$  is the distance between the two electrodes,  $t_s$  and  $w_s$  are the thickness and width of the membrane, and  $R$  is the resistance measured.

## Oxidative stability

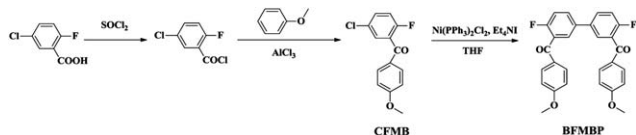
Oxidative stability was determined by soaking a membrane sample (10 × 10 mm<sup>2</sup>) in 50 mL of Fenton's reagent (3% H<sub>2</sub>O<sub>2</sub> containing 2 ppm FeSO<sub>4</sub>) at 80 °C for 1 h. The residue was then taken out, washed with water, and dried under vacuum at 100 °C until a constant weight (remaining weight).

## Results and discussion

### Synthesis of monomers and polymers

Scheme 1 shows the synthetic route towards the monomer **BFMBP**. **CFMB** was firstly prepared by the aluminium chloride catalyzed Friedel-Crafts acylation of anisole with 5-chloro-2-fluorobenzoyl chloride. Due to electronic and steric effects, the substitution reaction selectively occurred at the *para*-position to the methoxyl group of anisole. The chemical structure of **CFMB** was confirmed by its <sup>1</sup>H NMR, <sup>13</sup>C NMR (Fig. 1) and IR spectra.

NiBr<sub>2</sub> and triphenylphosphine (PPh<sub>3</sub>) were used as the catalyst and ligand for the nickel-catalyzed coupling reaction, respectively. The reaction proceeded well in DMAc, DMF and THF, however, the yield for the final product was only 10–20%, which might be due to the moisture-sensitive catalyst. Thus, a more stable catalyst of Ni(PPh<sub>3</sub>)<sub>2</sub>Cl<sub>2</sub> was instead investigated and the temperature was maintained under the mild condition of 50 °C. The yield was improved to about 50% after recrystallization from ethanol. Unlike many reported nickel-mediated reactions, which provided almost quantitative yields of the coupling products from various



**Scheme 1** Synthetic route towards monomer **BFMBP**.

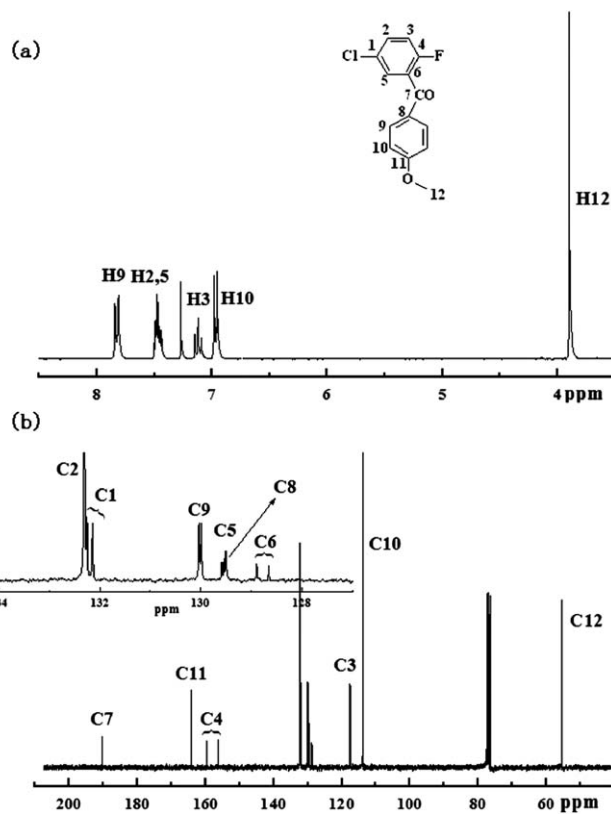


**Fig. 1** <sup>1</sup>H and <sup>13</sup>C NMR spectra of **CFMB** in CDCl<sub>3</sub>.

aryl halides,<sup>27,28</sup> the relatively negative results in this study might be attributed to the low reactivity of the precursor monomer **CFMB**. A carbonyl group was substituted at the *meta*-position toward the chloride group, which made it less reactive than some other chloride groups at the *ortho*-/*para*-positions toward the electron-withdrawing groups. The same phenomenon was also found by D. K. Taylor's group.<sup>29</sup> The chemical structure of **BFMBP** was confirmed by its <sup>1</sup>H NMR, <sup>13</sup>C NMR (Fig. 2) and IR spectra. On the one hand, the chemical shifts of the two protons *ortho* to the chloride (H2 and H5 in Fig. 1a,  $\delta = 7.47$ – $7.40$  ppm) shifted to the low field ( $\delta = 7.66$ – $7.62$  ppm) in Fig. 2a. On the other hand, the peak assigned to the carbon atom C1 ( $\delta = 132.25$  and  $132.14$  ppm in Fig. 1b) also shifted to  $135.78$  and  $135.74$  ppm, respectively, in Fig. 2b. These results provide obvious evidence for the phenyl-phenyl bond formation.

Scheme 2 shows the synthetic route towards polymers **4**. Polymers **2** were first obtained by the aromatic nucleophilic substitution polycondensation in the presence of K<sub>2</sub>CO<sub>3</sub>. Although two of the three counterpart (dihydroxy) monomers chosen in this study have rigid rod structures (**a** and **b**), no precipitation occurred during the polymerization reactions. The results of the polymerization reactions are summarized in Table 1. The number-average molecular weights ( $M_n$ ) and polydispersity indices (PDIs) of polymers **2** were in the range of  $3.1$ – $4.3 \times 10^4$  and  $2.0$ – $2.4$ , respectively. Polymers **2** showed good solubilities in common organic solvents such as CHCl<sub>3</sub>, CH<sub>2</sub>Cl<sub>2</sub>, DMSO, DMAc, *etc.* The chemical structures of polymers **2** were confirmed by their <sup>1</sup>H NMR and FTIR spectra. The relative

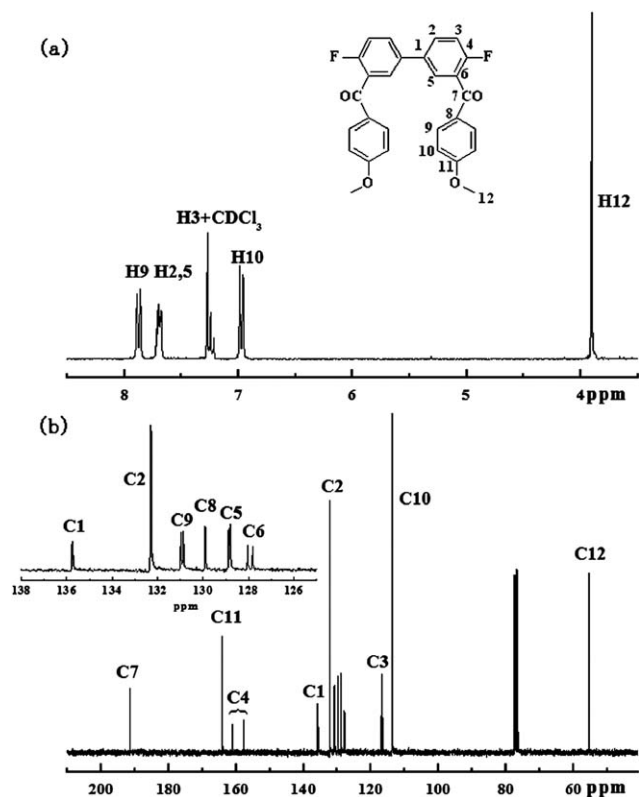
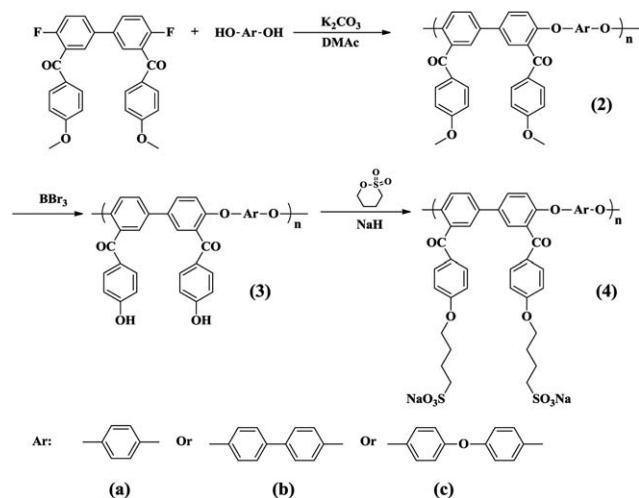


Fig. 2  $^1\text{H}$  and  $^{13}\text{C}$  NMR spectra of BFMBP in  $\text{CDCl}_3$ .



Scheme 2 Synthetic route towards the sulfonated polymers 4.

Table 1 Synthesis of polymers 2

Code	$M_n^a$ (kDa)	$M_w^a$ (kDa)	PDI <sup>a</sup>
2a	31	74	2.4
2b	43	85	2.0
2c	35	77	2.2

<sup>a</sup> Determined by GPC eluted with DMF using a polystyrene standard.

intensities of the aromatic-H to methoxy-H were 3.09, 3.78 and 3.67 for polymers 2a, 2b and 2c, respectively, close to the theoretical values of 3.00, 3.67 and 3.67, respectively (see Fig. S1 in the ESI†). The IR spectra of polymers 2 exhibited characteristic absorptions around 2960–2870, 1658, 1597, and 1169  $\text{cm}^{-1}$  due to the C–H, C=O, C=C and C–O–C stretchings, respectively. Polymers 2 were then converted to polymers 3 by treatment with  $\text{BBr}_3$ . In the  $^1\text{H}$  NMR spectra of polymers 2b and 3b, the characteristic methoxy protons at 3.82 ppm of polymer 2b have completely disappeared, and hydroxy proton signals appear at 10.36 ppm, as shown in Fig. S2.† Finally, the SPPEs, 4, were obtained by the reaction of the resulting polymers 3 with 1,4-butanedisulfone in the presence of sodium hydride.

The chemical structures of polymers 4 were also confirmed by FTIR and  $^1\text{H}$  NMR spectroscopies. The IR spectra of polymers 4 showed characteristic absorptions corresponding to the C=O and C=C stretchings around 1658 and 1600  $\text{cm}^{-1}$ , whereas the typical O=S=O stretching was observed at around 1115 and 1050  $\text{cm}^{-1}$  (Fig. S3†). The  $^1\text{H}$  NMR spectra of polymers 4 are shown in Fig. 3. New peaks at around 4.01, 3.91 and 3.89 ppm were assigned to the  $\alpha$ -methylene protons next to the phenoxy groups for 4a, 4b and 4c, respectively, indicating the introduction of long sulfoalkyl side chains. Since the typical signals of the  $\alpha$ -methylene protons next to the  $-\text{SO}_3\text{Na}$  groups overlapped with the  $\text{DMSO}-d_6$  peak, the  $\text{IEC}_{\text{NMR}}$  values were calculated by the relative intensities of the methylene protons to the aromatic protons. All the data were close to the theoretical values, which suggested the well-controlled nucleophilic reaction of polymers 3 with 1,4-butanedisulfone (Table 2).

### Thermal properties and oxidative stability

The thermal properties of polymers 4 in the acid form were evaluated by TGA and DSC. No obvious glass transition temperatures  $T_g$ s could be observed in all the polymers 4. Fig. 4 shows the TGA curves of polymers 4 in  $\text{N}_2$  and the weight loss temperatures are listed in Table 2. All the polymers 4 exhibited  $T_{d,5\%}$  values over 244  $^\circ\text{C}$ , which could satisfy the requirement

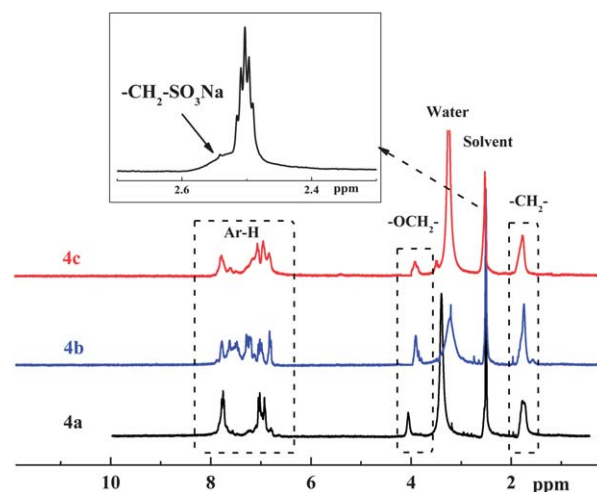


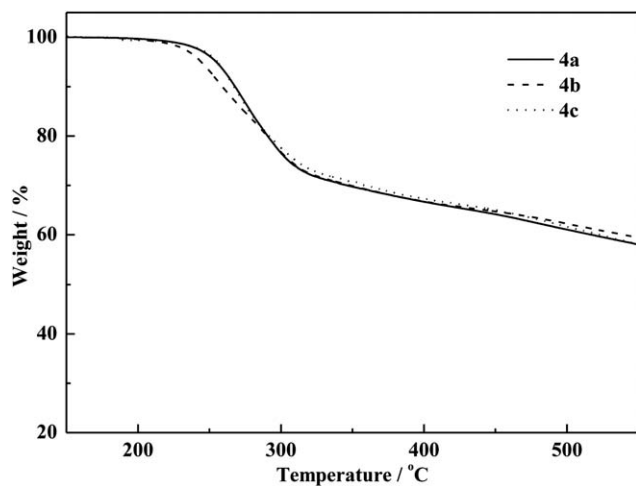
Fig. 3  $^1\text{H}$  NMR spectra of polymers 4a, 4b and 4c in  $\text{DMSO}-d_6$ .

**Table 2** Physical properties of polymers **4**

		<b>4a</b>	<b>4b</b>	<b>4c</b>
IEC <sub>cal</sub>	(mequiv. g <sup>-1</sup> )	2.59	2.36	2.31
IEC <sub>NMR</sub>	(mequiv. g <sup>-1</sup> )	2.51	2.19	2.10
IEC <sub>titr</sub>	(mequiv. g <sup>-1</sup> )	2.45	2.08	1.96
T <sub>d,5%</sub>	(°C)	257.4	244.2	254.2
T <sub>d,10%</sub>	(°C)	268.0	259.0	265.3
50% RH <sup>a</sup>	Δ <i>l</i> <sub>c</sub>	0.021	0.014	0.010
	Δ <i>t</i> <sub>c</sub>	0.030	0.020	0.020
70% RH <sup>a</sup>	Δ <i>l</i> <sub>c</sub>	0.060	0.048	0.040
	Δ <i>t</i> <sub>c</sub>	0.090	0.070	0.050
95% RH <sup>a</sup>	Δ <i>l</i> <sub>c</sub>	0.110	0.102	0.070
	Δ <i>t</i> <sub>c</sub>	0.130	0.120	0.090
RW <sup>b</sup>	(%)	81	90	94

<sup>a</sup> Dimensional changes of SPPEs at 80 °C. Δ*l*<sub>c</sub> and Δ*t*<sub>c</sub> refer to the changes in plane and through plane directions, respectively.

<sup>b</sup> Remaining weight; measured by soaking the membranes in Fenton's reagent (3% H<sub>2</sub>O<sub>2</sub> containing 2 ppm FeSO<sub>4</sub>) at 80 °C for 1 h.

**Fig. 4** TGA curves of SPPEs.

for medium-temperature fuel cells. There is an apparent weight loss starting from 220 to 300 °C, which is close to the theoretical values for the decomposition of the sulfonic acid groups in the side chains. The second weight loss step is observed from 300 to 550 °C, attributable to the cleavage of the alkyl side chains.

The oxidative stability of the SPPE membranes was evaluated by the remaining weight in Fenton's reagent (3% H<sub>2</sub>O<sub>2</sub> aqueous solution containing 2 ppm FeSO<sub>4</sub>) at 80 °C for 1 h, and these results are listed in Table 2. All the membranes showed an excellent oxidative stability with a remaining weight greater than 81%. Since it is widely considered that the electron-donating groups (-O-) in the *ortho*- and *para*-positions to the sulfonic acid group may lead to a lower oxidative stability, the sulfonated aliphatic side chains would contribute to the high oxidative stabilities of the SPPEs.<sup>20</sup>

### Mechanical properties

The dynamic mechanical properties were investigated by DMA measurements. Fig. S4† shows the storage modulus (*E'*) and loss

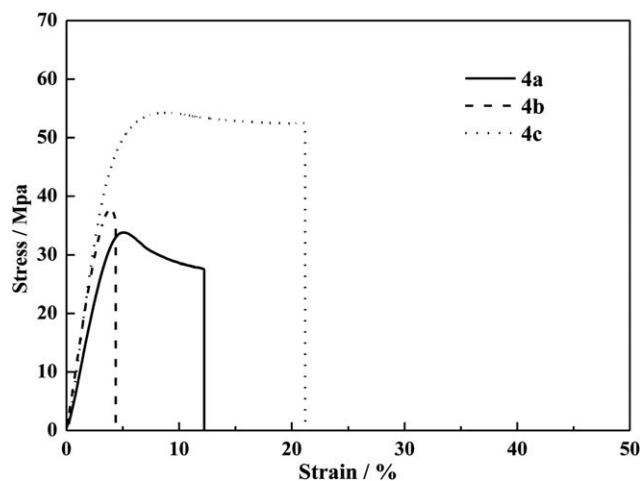
modulus (*E''*) of **4c** as a function of temperature. The *E'* and *E''* values of 2.6 GPa and 300 MPa are maintained from 80 to 180 °C, respectively, indicating the excellent mechanical strength despite the relatively high IEC value (1.96 mequiv. g<sup>-1</sup>).

Typical tensile stress-strain curves of all the SPPE membranes are shown in Fig. 5. They exhibited a reasonably high mechanical strength with a Young's modulus (*M*), maximum stress (*S*) and elongation at break (*E<sub>b</sub>*) values ranging from 1.01 to 1.30 GPa, 34–54 MPa and 4.4–21.2%, respectively, which indicated that the membranes could undergo a fairly large deformation or sustain a quite high external impact without breaking in practical applications. Polymer **4c** exhibited the highest values of 1.30 GPa, 54 MPa and 21.2% for the *M*, *S* and *E<sub>b</sub>*, respectively, which might indicate that the appropriate level of rigidity for the polymer backbone can improve the mechanical strength for these types of PEMs. The free rotation of ether linkages between aromatic groups of **4c** should cause the higher elasticity compared to others, and thereby its mechanical properties such as tensile strengths could also be improved.

### IEC, WU and dimensional change

The IEC values were determined by a back-titration method, and the results are listed in Table 2. All the titrated data were close to the calculated ones from the <sup>1</sup>H NMR spectra, indicating a complete proton exchange process.

As is well known, the WU of the PEMs has a significant effect on the membrane conductivity. Water molecules usually facilitate the proton transfer; however, an excessive WU would inevitably lead to an undesirable membrane swelling, resulting in a reduced mechanical strength of the membrane. Fig. 6 shows the WU of polymers **4** as a function of the relative humidity, together with that of Nafion 117 for comparison. Analogous to the common aromatic sulfonated polymers, the WUs of polymers **4** showed a greater RH dependence than that of Nafion, especially under a high RH condition. Regardless of the similar IEC values, the WU of **4c** is 30% lower than **4b** over the entire RH range, which indicates the better swelling behavior of the latter.

**Fig. 5** Stress-strain curves of SPPEs.

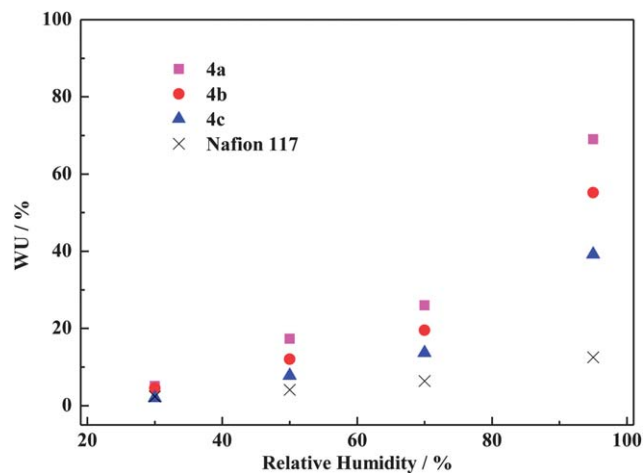


Fig. 6 WU of polymers 4 as a function of relative humidity.

The dimensional change data of polymers 4 are also summarized in Table 2. Compared to some other well-developed poly(phenylene)s or poly(ether sulfones)s, polymers 4 exhibit much lower dimensional changes.<sup>30–32</sup> The phenyl-phenyl bond increases the rigidity of the main chain, which may suppress the excessive swelling of the membranes even under high RH conditions. For example, polymer 4a with an IEC of 2.45 mequiv. g<sup>-1</sup> shows only 0.021 and 0.03 in-plane and through-plane directions under 50% RH, respectively, whereas 0.110 and 0.13 in-plane and through-plane directions under 95% RH, respectively. It is expected that polymer 4c displayed the best dimensional stability due to its lowest IEC values. Its  $\Delta l_c$  was 0.07 under 80 °C/95% RH, which would meet the requirement for a single cell test.

### Proton conductivity

Fig. 7 shows the proton conductivity of polymers 4 as a function of RH at 80 °C, together with that of Nafion 117 for comparison. All the polymers 4 exhibited a greater humidity dependence than that of Nafion. For example, polymer 4a with an IEC value of 2.45 exhibited the highest  $\sigma$  value of 237 mS cm<sup>-1</sup> under the 95% RH condition. It decreased to 8.5 mS cm<sup>-1</sup> with a decrease of RH to 30%, however, it was still slightly higher than that of Nafion (7.3 mS cm<sup>-1</sup>), indicating the better proton conductive capacity of the former.

The relationship between the WU and proton conductivity of polymers 4 and Nafion 117 was investigated. In Fig. 8, the  $\sigma$  value is plotted *versus* the hydration number,  $\lambda$ , which is the number of water molecules per a sulfonic acid unit. As could be seen, all the membranes tend to increase their proton conductivity with increasing  $\lambda$  values. At a similar proton conductivity level, polymers 4 have higher  $\lambda$  values than Nafion, indicating that polymers 4 require many more water molecules to facilitate proton transfer than the latter. Polymer 4a exhibits a higher proton conductivity compared to Nafion 117 over the entire range, probably due to its highest IEC value and well-connected proton pathways.

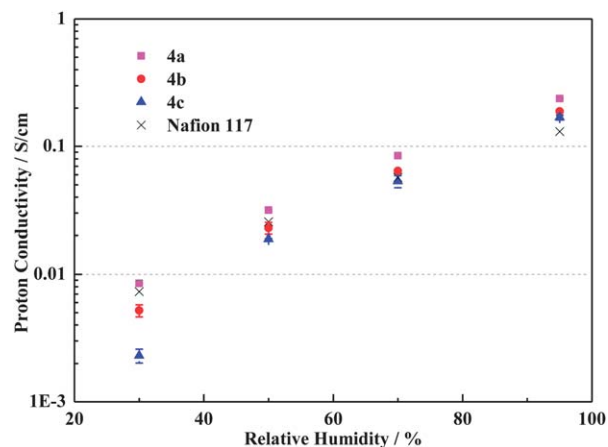


Fig. 7 Humidity dependence of proton conductivities of polymers 4 and Nafion 117 at 80 °C.

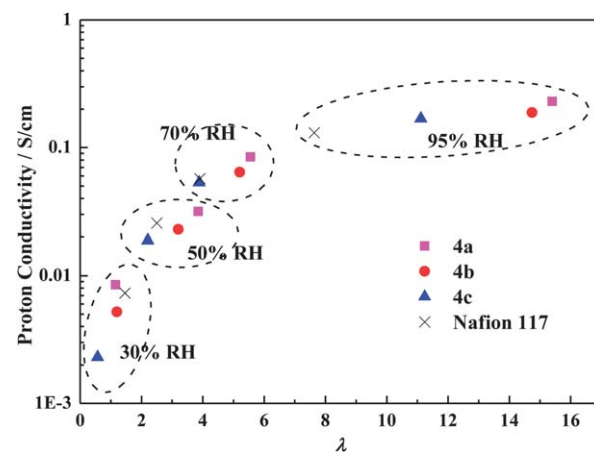
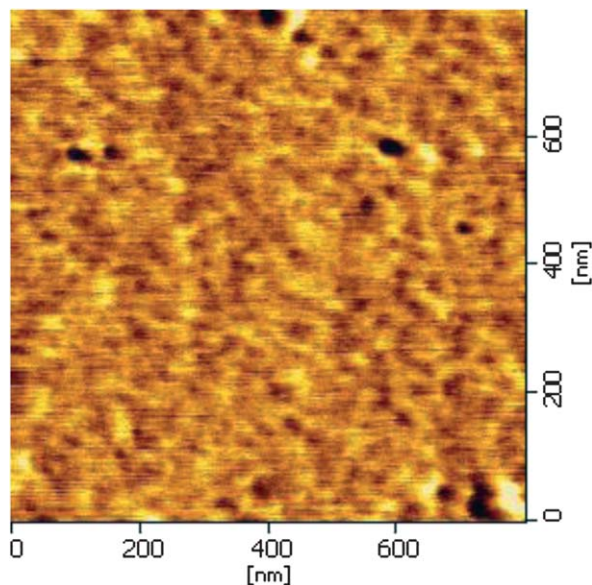


Fig. 8 Relationship between hydration number ( $\lambda$ ) and proton conductivity for polymers 4 and Nafion 117 at 80 °C.

### Morphology

The nanostructure and morphology of polymer 4a were studied using WAXD, SAXS and AFM. The same films in the dried and hydrated states were used for the WAXD and SAXS measurements. In both cases of the dried and hydrated films, the WAXD profiles showed a broadened reflection at around  $2\theta = 20^\circ$ , which corresponds to the intermolecular spacing of the benzene rings and/or alkyl chains with sulfonic acid. No reflections were observed in the SAXS profiles. These data suggest that the polymer 4a film has an amorphous state. The AFM tapping mode phase image of the 4a membrane was recorded under ambient conditions on an  $800 \times 800 \text{ nm}^2$  size scale to investigate its surface morphology. As can be seen in Fig. 9, a continuous phase-separated nanostructure was found in which the sulfonic acid groups aggregate to form the nano-channels structures (dark region in Fig. 9), although the direction of the structures is disordered. The formation of a phase-separated nanostructure, even disordered, may contribute to the efficient proton transport and excellent proton conductivity.



**Fig. 9** AFM tapping mode phase image of the **4a** membrane: scan size is  $800 \times 800 \text{ nm}^2$ .

## Conclusion

A series of PPEs with sulfonic acids *via* long alkyl side chains, SPPEs (polymers **4**), were successfully obtained by the polycondensation of **BFMBP** and various dihydroxy-monomers in the presence of  $\text{K}_2\text{CO}_3$ , followed by demethylation of polymers **2** with  $\text{BBr}_3$ , and finally by the reaction of the resulting polymers **3** with 1,4-butanediol. The titrated IEC values of the SPPEs were slightly lower than the theoretical and calculated ones from the  $^1\text{H}$  NMR spectra. The SPPEs exhibited high thermal stabilities despite the fully aliphatic side chains, excellent oxidative stabilities, and reasonably high mechanical strengths with a Young's modulus ( $M$ ), maximum stress ( $S$ ) and elongation at break ( $E_b$ ) values that ranged from 1.01 to 1.30 GPa, 34–54 MPa and 4.4–21.2%, respectively. The DMA results showed the high storage modulus of 2.6 GPa for **4c** from 80–180 °C, regardless of its relatively high IEC value of 1.96 mequiv.  $\text{g}^{-1}$ . All SPPEs exhibited a greater RH dependence than Nafion for the proton conductivities. Polymer **4a** with an IEC value of 2.45 mequiv.  $\text{g}^{-1}$  showed a high  $\sigma$  value of  $8.6 \text{ mS cm}^{-1}$  under 80 °C/30% RH conditions, whereas it was  $7.3 \text{ mS cm}^{-1}$  for Nafion 117. Consequently, the novel PPEs with pendant alkyl sulfonated side chains are promising candidates for fuel cell applications.

## Acknowledgements

This work is supported by the Industrial Technology Research Grant Program in 2011 (#11B02008c) from New Energy and Industrial Technology Development Organization (NEDO) of Japan.

## Notes and references

1 K. A. Mauritz and R. B. Moore, *Chem. Rev.*, 2004, **104**, 4535.

- 2 O. J. Savadoga, *J. New Mater. Electrochem. Syst.*, 1998, **1**, 47.
- 3 M. Rikukawa and K. Sanui, *Prog. Polym. Sci.*, 2000, **25**, 1463.
- 4 A. H. Hickner, H. Ghassemi, Y. S. Kim, B. R. Einsla and J. E. McGrath, *Chem. Rev.*, 2004, **104**, 4587.
- 5 (a) S. Takamuku and P. Jannasch, *Adv. Energy Mater.*, 2012, **2**, 129; (b) The 2011 Progress Report for US DOE Hydrogen and Fuel Cells Program, [http://www.hydrogen.energy.gov/pdfs/progress11/v\\_c\\_1\\_hamrock\\_2011.pdf](http://www.hydrogen.energy.gov/pdfs/progress11/v_c_1_hamrock_2011.pdf); (c) M. Gebert, A. Ghielmi, L. Merlo, M. Corasaniti and V. Arcella, *ECS Trans.*, 2010, 279.
- 6 T. Higashihara, K. Matsumoto and M. Ueda, *Polymer*, 2009, **50**, 5341.
- 7 C. H. Park, C. H. Lee, M. D. Guiver and Y. M. Lee, *Prog. Polym. Sci.*, 2011, **36**, 1443.
- 8 Y. L. Liu, *Polym. Chem.*, 2012, **3**, 1373.
- 9 H. Zhang and P. K. Shen, *Chem. Rev.*, 2012, **112**, 2780.
- 10 H. Zhang and P. K. Shen, *Chem. Soc. Rev.*, 2012, **41**, 2382.
- 11 K. Matsumoto, T. Higashihara and M. Ueda, *Macromolecules*, 2008, **41**, 7560.
- 12 X. Zhang, Z. Hu, L. Luo, S. Chen, J. Liu, S. Chen and L. Wang, *Macromol. Rapid Commun.*, 2011, **32**, 1108.
- 13 X. Zhang, S. Chen, J. Liu, Z. Hu, S. Chen and L. Wang, *J. Membr. Sci.*, 2011, **371**, 276.
- 14 K. Miyatake, Y. Chikashige, E. Higuchi and M. Watanabe, *J. Am. Chem. Soc.*, 2007, **129**, 3879.
- 15 K. Matsumoto, T. Higashihara and M. Ueda, *Macromolecules*, 2008, **42**, 1161.
- 16 B. Lafitte and P. Jannasch, *Adv. Funct. Mater.*, 2007, **17**, 2823.
- 17 C. Wang, D. W. Shin, S. Y. Lee, N. R. Kang, Y. M. Lee and M. D. Guiver, *J. Membr. Sci.*, 2012, **405–406**, 68.
- 18 Z. Hu, Y. Yin, K.-I. Okamoto, Y. Moriyama and A. Morikawa, *J. Membr. Sci.*, 2009, **329**, 146.
- 19 S. Seesukphronrarak and A. Ohira, *Chem. Commun.*, 2009, 4744.
- 20 X. Zhang, L. Sheng, T. Higashihara and M. Ueda, *Polym. Chem.*, 2013, **4**, 1235.
- 21 X. Zhang, Z. Hu, Y. Pu, S. Chen, J. Ling, H. Bi, S. Chen, L. Wang and K.-I. Okamoto, *J. Power Sources*, 2012, **216**, 261.
- 22 T. Xu, D. Wu and L. Wu, *Prog. Polym. Sci.*, 2008, **33**, 894.
- 23 Z. Zhang, L. Wu and T. Xu, *J. Membr. Sci.*, 2011, **373**, 160.
- 24 T. Xu, D. Wu, S.-J. Seo, J.-J. Woo, L. Wu and S.-H. Moon, *J. Appl. Polym. Sci.*, 2012, **124**, 3511.
- 25 K. Miyatake, H. Zhou and M. Watanabe, *J. Polym. Sci., Part A: Polym. Chem.*, 2005, **43**, 1741.
- 26 L. Sheng, T. Higashihara, S. Nakazawa and M. Ueda, *Polym. Chem.*, 2012, **3**, 3289.
- 27 M. Iyoda, H. Otsuka, K. Sato, N. Nisato and M. Oda, *Bull. Chem. Soc. Jpn.*, 1990, **63**, 80.
- 28 I. Colon and D. R. Kelsey, *J. Org. Chem.*, 1986, **51**, 2627.
- 29 B. D. Koepnick, J. S. Lipscomb and D. K. Taylor, *J. Phys. Chem. A*, 2010, **114**, 13228.
- 30 X. Zhang, Z. Hu, S. Zhang, S. Chen, S. Chen, J. Liu and L. Wang, *J. Appl. Polym. Sci.*, 2011, **121**, 1707.
- 31 K. Nakabayashi, T. Higashihara and M. Ueda, *J. Polym. Sci., Part A: Polym. Chem.*, 2010, **48**, 2757.
- 32 K. Nakabayashi, K. Matsumoto, T. Higashihara and M. Ueda, *Polym. J.*, 2009, **41**, 332.